Highly Linear Reconfigurable Mixer Designed for Environment-Aware Receiver

Mohammad-Mahdi Mohsenpour* and Carlos E. Saavedra†
Department of Electrical and Computer Engineering
Queen's University, Kingston, ON, Canada
Email: *m.mohsenpour@queensu.ca, †Saavedra@queensu.ca

***Abstract*—A 4-state, highly linear, reconfigurable mixer is presented in this paper. The proposed mixer is an essential part of the environment-aware receiver, introduced in this article. A set of switches are used in the LO and IF stages of the mixer to digitally tune the linearity of the mixer in exchange for lower power consumption. Three sets of cross-coupled pairs are utilized in the mixer to dynamically inject the proper current into the mixer and improve the linearity of each state of the mixer. The proposed mixer is designed using a standard 130-nm CMOS process. The mixer delivers 10, 6.2, 1.8, and -2.9 dBm of third-order intercept point (IIP3) while the average NF is 9.3 dB and varies only 1 dB in different states. Conversion gain of the mixer varies within 16.8 to 7.8 dB in 0.5 to 7 GHz. The mixer consumes 2.4 to 9.6 mW from a 1.2V supply.**

***Index Terms*—Reconfigurable Mixer, Environment-Aware Receiver, CMOS Active Mixer, High Linearity**

I. Introduction

Continued device miniaturization, achieved by advances in the semiconductor industry and sub-micron technologies in last decades, continuously challenges the industry with new and aggravated problems regarding die yield loss and testing due to higher process, voltage, and temperature (PVT) variations.

The on-going research on Built-in self-test (BIST) methods is one of the primary solutions to increasingly high measurement costs [1]–[5]. In BIST, the required circuits, necessary to test functionality and particular merits of each chip, is integrated with it, which leads to fast and inexpensive testing. Fast, on-chip measurement of different parameters and metrics of components makes self-healing possible [1], [3]–[7]. Therefore, the chip's performance can be tuned back to its optimum and consequently improve the die yield, reduce the design margins, compensate for PVT variations, device aging.

BIST and self-healing methods operate off-line or in time periods when the receiver or transmitter are not receiving or sending any signal while remaining idle in on-line mode. In this article, the idea of BIST and self-healing is expanded to form an *environment-aware* receiver. In the proposed architecture, the built-in test measures the power spectrum of the desired channel and all other channels of the communication band. This data is being used to estimate the minimum required parameters of the receiver to receive the desired signal with determined quality and speed. Consequently, the receiver's front-end adaptively tunes to meet the estimated parameters while using the resources, such as power, more efficiently. Here, the required linearity of the receiver is estimated, and a highly linear reconfigurable mixer is proposed as the means to adaptively tune the receiver's linearity.

II. Environment-Aware Receiver Architecture

Figure 1 shows the proposed environment-aware receiver along with the auxiliary test path. The received signal is fed to the auxiliary path through a weak coupling coefficient to ensure negligible effect on the main receiving path. Therefore the auxiliary signal's path, P_{aux} is considerably smaller compared to the main path's signal, P_{in}. Consequently, the required linearity metrics such as P_{1dB} and IIP3 are more relaxed in the auxiliary path. P_{aux} is feeding a passive mixer directly which demonstrates better linearity compared to its active counterparts. Passive mixers, intrinsically, have higher NF and negative conversion gain, but their zero power consumption, small sizes make them very attractive for the auxiliary path, to minimize the power and size overhead cost to the receiver. Also, channels with weak signal levels affect the estimations of the performance metrics of the receiver such as P_{1dB} and IIP3, insignificantly.

P_{aux} is fed to the mixer, driven by a local oscillator, and passes through a low-pass, channel select filter. To measure the power carried in each channel a power detector is placed after the down conversion. By tuning the LO signal to the center frequencies of different channels, the received signal's power spectrum can be monitored and stored for further analysis.

After performing the analysis on the detected power and determining the required overall metrics for the receiver, the control signal will be sent to the main receiver's components such as LNA, mixer, and the local oscillator, to adjust their performance in accordance. Therefore, the receiver can receive the desired signal and optimize its power consumption at each moment and according to present signals in channels of the receive frequency band or any changes in it.

Every aspect of receiver's performance should be analyzed, and the required metrics need to be estimated. In this paper, the focus is on the estimation of the linearity, which is provided in the next section.

III. Estimation of the Required Linearity Performance of the Receiver

A sample power spectrum of different channels in a communication band is shown in Fig. 1. Here, the modulated power

978-1-4673-6853-7/17/$31.00 ©2017 IEEE

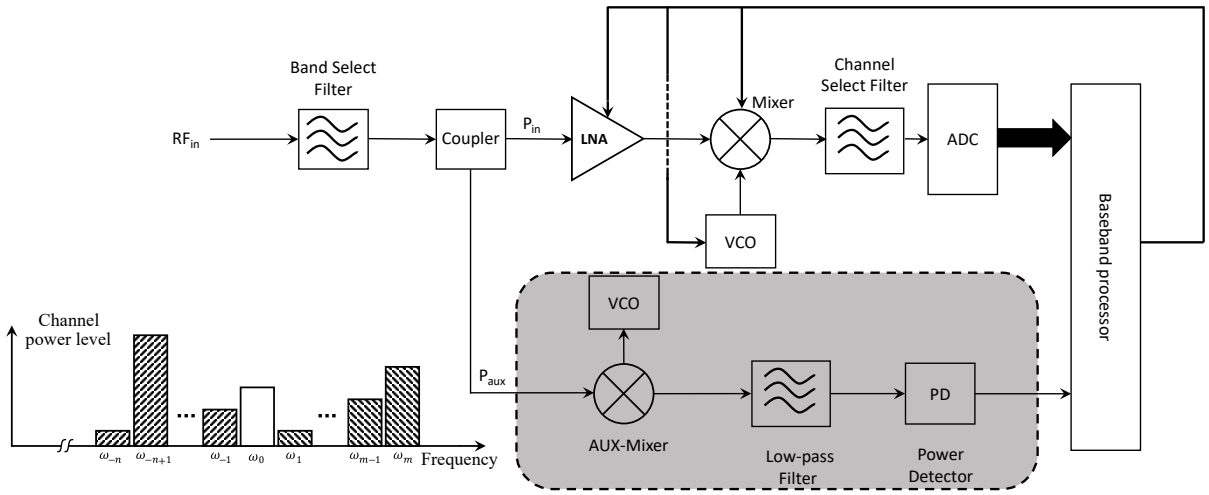

Fig. 1. Block diagram of the proposed environment-aware receiver with its auxiliary path and a sample estimated power spectrum of the received signal.

of each channel is shown by a constant power level distributed over the entire channel bandwidth. As it is used in performing the two-tone test and compression test of RF components and receivers, it is also a reasonable approximation to condense each channel's energy to single tones at their carrier frequencies and with equal powers, demonstrated by A_i.

$$x(t) = A_0 \cos\omega_0 t + \sum_{\substack{i=-n \\ i\neq 0}}^{m} A_i \cos\omega_i t \tag{1}$$

Equation (1) is used here to approximate the input signal of a receiver which is receiving the desired signal from the channel with the carrier frequency of ω_0. The frequencies $\omega_{\pm i}$ also demonstrates the carrier frequencies of other channels, placed to the right $(+)$ and left $(-)$ of the desired channel. Considering third-order non-linearity characteristics for the receiver, the output signal can be estimated by

$$y(t) = \alpha_1 x(t) + \alpha_2 x^2(t) + \alpha_3 x^3(t), \tag{2}$$

where the α_1, α_2, and α_3 are the system's overall gain, second order, and third order non-linearity coefficients, respectively.Therefore, the signals available in non-desired channels corrupts the desired signal, carried at ω_0, and passes through the channel select filter of the receiver. The output terms present at ω_0 consist of the amplified desired signal and third order intermodulation products.

$$y(t) = \left\{\alpha_1 A_0 + \frac{3}{4}\alpha_3 \left(C_1 + C_2 + C_3\right)\right\} \cos\omega_0 t + \ldots \tag{3}$$

In (3), all the intermodulation terms at frequency of ω_0 are extracted from the rest of the terms. C_1, C_2, and C_3 represent the intermodulation products, consist of one to three different channels' signals and are given by (4) to (6), respectively.

$$C_1 = A_0^3 + 2A_0 \sum_{\substack{i=-n \\ i\neq 0}}^{m} \left(A_i^2\right) \tag{4}$$

$$\begin{aligned} C_2 = &\sum_{\substack{i=\lceil \frac{-n}{2} \rceil \\ i\neq 0}}^{\lfloor \frac{m}{2} \rfloor} \left(A_i^2 \times A_{2i}\right) + \sum_{\substack{i=L_{\min} \\ i\neq 0}}^{L_{\max}} \left(A_i^2 \times A_{-2i}\right) \\ &+ 4A_0 \sum_{i=1}^{\min(m,n)} \left(A_i \times A_{-i}\right) \\ &L_{\min} = \min\left(-n, \lfloor \frac{m}{2} \rfloor\right), L_{\max} = \max\left(m, \lceil \frac{n}{2} \rceil\right) \end{aligned} \tag{5}$$

$$\begin{aligned} C_3 = &2 \sum_{i=-n}^{-1} \sum_{\substack{j= \\ -(n+i)}}^{m} \left(A_i \times A_j \times A_{i+j}\right) \\ &+ 2 \sum_{i=1}^{\lfloor \frac{m-1}{2} \rfloor} \sum_{\substack{j= \\ i+1}}^{m-i} \left(A_i \times A_j \times A_{i+j}\right) \end{aligned} \tag{6}$$

where $\lfloor\cdot\rfloor$ and $\lceil\cdot\rceil$ denote the `floor` and `ceil` functions, respectively.

Depending on the number of occupied channels, specially those with significant power levels the intermodulation terms can vary significantly. As shown on (7), in order to adaptively maintain the intermodulation terms X_{margin} dB lower than the desired signal, the receivers linearity needs to be tuned adaptively as well. The required α_1 to α_3 ratio, given in (8), plays an essential role in estimating the overall required IIP3 and $P_{1\text{dB}}$ of the receiver in (9) and (10), respectively.

$$20\log\left|\alpha_1 A_0\right| - X_{\text{margin}} = 20\log\left|\frac{3}{4}\alpha_3\left(C_1 + C_2 + C_3\right)\right| \tag{7}$$

$$\frac{4}{3}\left|\frac{\alpha_1}{\alpha_3}\right| = 10^{X_{\text{margin}}/20} \times \frac{C_1 + C_2 + C_3}{A_0} \tag{8}$$

$$IIP_3|_{\text{dB}} = 20\log\sqrt{\frac{4}{3}\left|\frac{\alpha_1}{\alpha_3}\right|} \tag{9}$$

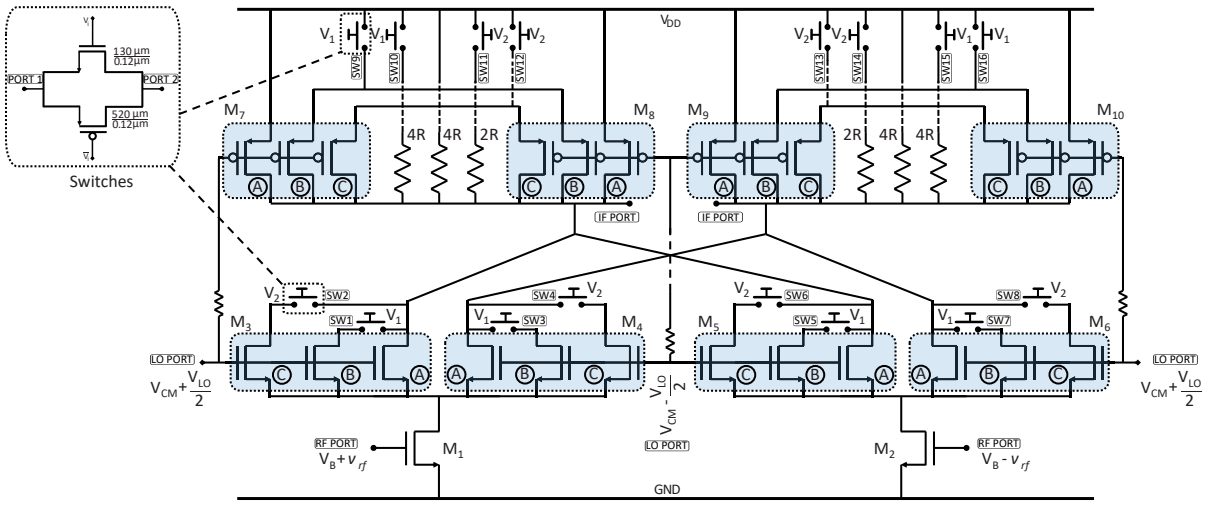

Part	$\left(\frac{W}{L}\right)_{1,2}$	$\left(\frac{W}{L}\right)_{(3-6)_A}$	$\left(\frac{W}{L}\right)_{(3-6)_B}$	$\left(\frac{W}{L}\right)_{(3-6)_C}$	$\left(\frac{W}{L}\right)_{(7-10)_A}$	$\left(\frac{W}{L}\right)_{(7-10)_B}$	$\left(\frac{W}{L}\right)_{(7-1)_C}$	R
Value	$\frac{32.8\ \mu m}{0.12\ \mu m}$	$\frac{20\ \mu m}{0.12\ \mu m}$	$\frac{40\ \mu m}{0.12\ \mu m}$	$\frac{40\ \mu m}{0.12\ \mu m}$	$\frac{210.1\ \mu m}{1\ \mu m}$	$\frac{220\ \mu m}{1\ \mu m}$	$\frac{370\ \mu m}{1\ \mu m}$	500 Ω

Fig. 2. Schematic of the proposed reconfigurable mixer with cross-coupling pairs for linearity improvement and the tuning switches.

TABLE I
ACTIVE DEVICES IN DIFFERENT MODES OF THE MIXER.

State	V_2	V_1	V_B	I_{eff}	Active Devices	R_{eff}
S_1	0	0	0.53	$0.25I_{\max}$	A	4R
S_2	0	1.2	0.61	$0.5I_{\max}$	A+B	2R
S_3	1.2	0	0.67	$0.75I_{\max}$	A+C	$\frac{4}{3}$R
S_4	1.2	1.2	0.73	$I_{\max}$	A+B+C	R

$$P_{\text{1dB}} = 20\log\sqrt{0.145\left|\frac{\alpha_1}{\alpha_3}\right|} \tag{10}$$

A_is in (3)-(8) are being measured by the auxiliary path of the receiver. Weakly coupled signal in the auxiliary path is addressed by (11) where A_{coupler} is the coupling coefficient.

$$x_{\text{AUX}}(t) = B_0\cos\omega_0 t + \sum_{\substack{i=-n \\ i\neq 0}}^{m} B_i\cos\omega_i t$$
$$B_i = A_i A_{\text{coupler}} \tag{11}$$

Use of passive mixer which inherently provides high linearity and also attenuating the signal significantly in the input of this path provides the power detector with each channels signal with little discrepancy. The detected power in the i$^{\text{th}}$ channel, P_i, is

$$P_i = 20\ \log\left(A_i A_{\text{coupler}} A_{\text{AUX}}\right) \tag{12}$$

where A_{AUX} is the loss coefficient imposed to the signal by the auxiliary path's components such as the passive mixer. Therefore, A_i can be estimated by

$$A_i \approx \frac{10^{P_i/20}}{A_{\text{coupler}} A_{\text{AUX}}}. \tag{13}$$

IV. RECONFIGURABLE MIXER DESIGN

In receiver front-end, the mixer's IIP3 is usually the bottleneck and the limiting factor of the receiver's overall IIP3. Because of the gain of the preceeding amplifier stage. changing IIP3 and P_{1dB} of the mixer affects the receiver linearity and sensitivity more substantially compared to the LNA's. Therefore, a reconfigurable mixer has been designed to modify the overall receiver's linearity accordingly.

Figure 2 depicts the proposed reconfigurable active mixer. The reconfigurable of the mixer is accomplished by scaling the current consumption of the mixer in the transconductance stage of the mixer along with proper scaling of LO and IF stages components. The transconductance stage is biased by V_{B} while v_{rf} denotes the input RF signal. The bias voltage and the LO signal of the switching stage are indicated by V_{CM} and V_{LO}, respectively.

The mixer employs pMOS cross-coupling pairs, provided by M_7-M_{10}, to dynamically inject current into the LO stage transistors, M_3-M_6. In LO zero-crossing instances, the injected current is minimal, and the load resistors provide the majority of the current to the LO stage. By increasing the LO signal's amplitude, in each period, the overdrive voltages of M_7-M_{10} also change accordingly to avoid excessive current through the load resistors, which consequently alleviates the gain compression in the output. This mixer is a reconfigurable variant of our previous works which is described in detail in [8].

As shown in Fig. 2, each of M_3-M_{10} and load resistors are divided into three parts to form a four state reconfigurable mixer. The mixer changes its behavior between its states through switches, SW1 - SW16, which are fed by two digital signals, V_1 and V_2. The switches are kept to a simple

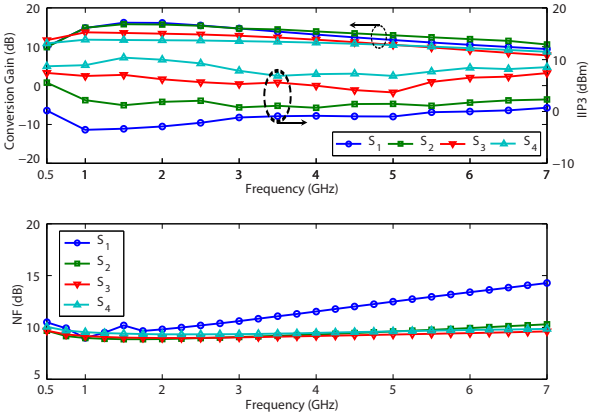

Fig. 3. Post-layout simulation result for NF (-NF is plotted), conversion gain, and IIP3 of the proposed mixer in four settings versus Frequency. $F_{\text{IF}} = 200$ MHz, $F_{\text{LO}} = F_{\text{RF}} + F_{\text{IF}}$, and $P_{\text{LO}} = 4$ dBm.

implementation of nMOS-pMOS pairs shown in the inset of Fig. 2.

In the lowest Linear state, S_1, all the switches are off and only $M_{(3-10)_A}$ are operating. The effective current of the mixer, I_{eff}, is $\frac{1}{4}I_{\max}$, where $I_{\max}$ is the maximum power consumption of the mixer in the highest linear state, S_4. Although the transconductance of M_{1-2} is minimum in S_1, the increase of the effective load resistor compensates for conversion gain and noise figure (NF) degradations. Table I shows the active devices in each of the mixers states, S_{1-4}, and shows how $I_{\text{eff}} \times R_{\text{eff}}$ is constant in all the states of the mixer to maintain M_{1-6} in saturation and avoid linearity degradation in the IF stage.

V. Simulation Results

The proposed mixer is designed with a maximum current budget of 8 mA, using the Global Foundries (formerly IBM) $0.13-\mu$m RF CMOS process and the components value are shown in Fig. 2. The post-layout simulation results of the mixer show a maximum power consumption of 9.6 mW from a 1.2 V supply for S_4. The chip core occupies an area of 0.08mm^2 ($300\mu\text{m}\times250\mu\text{m}$).

The post-layout simulation results for NF, conversion gain, and IIP3 of the mixer in different modes are depicted in Fig. 3. When $f_{\text{LO}} = 2$ GHz and $f_{\text{RF}} = 2.2$ GHz, The mixer tunes IIP3 to -2.89, 1.85, 6.21, and 10 dBm for S_{1-4}, respectively while its NF is 9.3 ± 0.5. Also, for $f_{\text{LO}} = 0.5$ to 7 GHz, the IIP3 is -1.41 ± 2.14, 3.14 ± 2.43, 5.56 ± 1.88, and 9.47 ± 0.92 for these states.

As is shown in Fig. 3, the conversion gain is between 16.8 dB and 7.8 dB on 0.5 GHz to 7 GHz, while the Bandwidth decreases from 6.5 GHz to 3.25 GHz by moving toward less linear modes. The conversion gain for the modes with less linear modes is higher and degrades faster with frequency due to the reduction of the LO-switches' transconductance. While the NF does not suffer much from this effect and is almost constant for lower frequencies, the discrepancy increases dramatically in higher frequencies for S_1. NF is 9.8 ± 0.9 dB for S_{2-4} but it reaches 15 dB at 7 GHz for S_1. A summary of the simulation results and a comparison with recent works [8]–[10] are provided in Table II.

TABLE II
Performance Summary and Comparison Table

	units	**This Work***	**[8]**	**[9]**	**[10]**
RF Freq.	GHz	0.5–7	0.5–6.5	0.3-1.2	1–10
Gain	dB	12.3 ± 4.5	10	8.8	3–8
Input $P_{1\text{dB}}$	dBm	-16 – -3.46	-2.4	-11±2.2	-14.1±1.9
IIP3	dBm	-3.55–10.35	9.52	-2.5±1.7	-5.5±1.5
DSB NF	dB	8.9–15.1	13	<4.8	8.3–12
DC power	mW	2.4–9.6	4.5	24	8.4
Chip area	mm^2	0.08	0.015	0.56	0.28

* Simulation results.

VI. Conclusion

Reconfigurable mixers are crucial and attractive for environment-aware receivers, which is introduced, and its required linearity estimation is analyzed here. Reconfigurable LO stage, IF loads, pMOS cross-coupled pairs, and taking advantage of the dynamic current injection method are exploited in this work to provide a reconfigurable mixer with high linearity and boosted gain.

References

[1] A. Banerjee and A. Chatterjee, "Signature driven hierarchical post-manufacture tuning of RF systems for performance and power," *IEEE Transactions on Very Large Scale Integration (VLSI) Systems*, vol. 23, no. 2, pp. 342–355, 2015.

[2] O. Inac, D. Shin, and G. M. Rebeiz, "A phased array RFIC with built-in self-test capabilities," *IEEE Transactions on Microwave Theory and Techniques*, vol. 60, no. 1, pp. 139–148, 2012.

[3] S. M. Bowers, K. Sengupta, K. Dasgupta, B. D. Parker, and A. Hajimiri, "Integrated Self-Healing for mm-Wave Power Amplifiers," *IEEE Transactions on Microwave Theory and Techniques*, vol. 61, no. 3, pp. 1301–1315, March 2013.

[4] D. C. Howard, P. K. Saha, S. Shankar, T. D. England, A. S. Cardoso, R. M. Diestelhorst, S. Jung, and J. D. Cressler, "A SiGe 8-18-GHz Receiver With Built-In-Testing Capability for Self-Healing Applications," *IEEE Transactions on Microwave Theory and Techniques*, vol. 62, no. 10, pp. 2370–2380, Oct 2014.

[5] P. K. Saha, D. C. Howard, S. Shankar, R. Diestelhorst, T. England, and J. D. Cressler, "A 6–20 GHz adaptive SiGe image reject mixer for a self-healing receiver," *IEEE Journal of Solid-State Circuits*, vol. 47, no. 9, pp. 1998–2006, 2012.

[6] C. Maxey, S. Raman, K. Groves, T. Quach, L. Orlando, A. Mattamana, G. Creech, and J. Rockway, "Mixed-Signal SoCs With In Situ Self-Healing Circuitry," *IEEE Design Test of Computers*, vol. 29, no. 6, pp. 27–39, Dec 2012.

[7] H. Wang, K. Dasgupta, and A. Hajimiri, "A broadband self-healing phase synthesis scheme," in *2011 IEEE Radio Frequency Integrated Circuits Symposium*. IEEE, 2011, pp. 1–4.

[8] M. Mohsenpour and C. E. Saavedra, "Method to Improve the Linearity of Active Commutating Mixers using Dynamic Current Injection," *IEEE Transactions on Microwave Theory and Techniques*, vol. 64, no. 12, pp. 4624–4631, 2016.

[9] S. He and C. E. Saavedra, "Design of a low-voltage and low-distortion mixer through Volterra-series analysis," *IEEE Transactions on Microwave Theory and Techniques*, vol. 61, no. 1, pp. 177–184, 2013.

[10] H. Zijie and K. Mouthaan, "A 1-to 10-GHz RF and Wideband IF Cross-Coupled Gilbert Mixer in 0.13 μm CMOS," *IEEE Transactions on Circuits and Systems II: Express Briefs*, vol. 60, no. 11, pp. 726–730, 2013.